Metabolism of phytol to phytanic acid in the mouse, and the role of PPARα in its regulation

J. Gloerich, D. M. van den Brink, J. P. N. Ruiter, N. van Vlies, F. M. Vaz, R. J. A. Wanders, and S. Ferdinandusse[1]

Laboratory of Genetic Metabolic Diseases, Departments of Clinical Chemistry and Pediatrics, Emma's Children's Hospital, Academic Medical Center, University of Amsterdam, 1105 AZ Amsterdam, The Netherlands

Abstract **Phytol, a branched-chain fatty alcohol, is the naturally occurring precursor of phytanic and pristanic acid, branched-chain fatty acids that are both ligands for the nuclear hormone receptor peroxisome proliferator-activated receptor α (PPARα). To investigate the metabolism of phytol and the role of PPARα in its regulation, wild-type and PPARα knockout (PPARα$^{-/-}$) mice were fed a phytol-enriched diet or, for comparison, a diet enriched with Wy-14,643, a synthetic PPARα agonist. After the phytol-enriched diet, phytol could only be detected in small intestine, the site of uptake, and liver. Upon longer duration of the diet, the level of the (*E*)-isomer of phytol increased significantly in the liver of PPARα$^{-/-}$ mice compared with wild-type mice. Activity measurements of the enzymes involved in phytol metabolism showed that treatment with a PPARα agonist resulted in a PPARα-dependent induction of at least two steps of the phytol degradation pathway in liver. Furthermore, the enzymes involved showed a higher activity toward the (*E*)-isomer than the (*Z*)-isomer of their respective substrates, indicating a stereospecificity toward the metabolism of (*E*)-phytol. In conclusion, the results described here show that the conversion of phytol to phytanic acid is regulated via PPARα and is specific for the breakdown of (*E*)-phytol.**—Gloerich, J., D. M. van den Brink, J. P. N. Ruiter, N. van Vlies, F. M. Vaz, R. J. A. Wanders, and S. Ferdinandusse. **Metabolism of phytol to phytanic acid in the mouse, and the role of PPARα in its regulation.** ***J. Lipid Res.*** **2007.** 48: **77–85.**

Supplementary key words peroxisome proliferator-activated receptor α • fatty aldehyde dehydrogenase • branched-chain fatty acids

Phytol is a branched-chain fatty alcohol (3,7,11,15-tetramethylhexadec-2-en-1-ol) that is abundantly present in nature as part of the chlorophyll molecule. The release of phytol from chlorophyll occurs effectively in the digestive system of ruminant animals only, presumably by bacteria present in the gut (1). As a result, a relatively high amount of free phytol is present in dairy products (2). In mammals, free phytol is readily absorbed in the small intestine and is metabolized to phytanic acid, a fatty acid that accumulates in a number of metabolic disorders. Increased levels of phytanic acid in the body are toxic, so this fatty acid needs to be broken down (3–9). Because the methyl-group at the 3 position prevents β-oxidation, phytanic acid first has to undergo a round of α-oxidation. This results in the formation of pristanic acid, which is one carbon atom shorter than phytanic acid and can be normally β-oxidized (10). A deficiency in α-oxidation, such as in Refsum disease, leads to increased levels of phytanic acid in plasma and tissues of patients, and this is thought to cause the main clinical symptoms of this disorder: retinitis pigmentosa, peripheral neuropathy, and cerebellar ataxia (3, 4). Because the breakdown of phytol will contribute to the phytanic and pristanic acid levels in these patients, it is important to study its metabolism and regulation.

In many animal studies, phytol is used as a precursor of phytanic acid. Addition of phytol to the diet results in an increase of phytol metabolites in tissues and plasma (6, 11–13). This has been used as a model to study the effects of the accumulation of phytol metabolites on fatty acid metabolism, in particular via the activation of the nuclear hormone receptor peroxisome proliferator-activated receptor α (PPARα), which is an important transcription factor in the regulation of fatty acid metabolism. Both phytanic and pristanic acid have been shown to activate PPARα in vitro (14, 15), and more recently, PPARα was also shown to be activated in vivo in mice fed a phytol-enriched diet (13).

Figure 1 shows a schematic representation of the metabolism of phytol to phytanic acid and the enzymes involved. First, phytol is converted into phytenal via a yet unknown alcohol dehydrogenase, and subsequently, phytenal is converted into phytenic acid by the microsomal

Manuscript received 31 January 2006 and in revised form 16 May 2006 and in re-revised form 7 June 2006 and in re-re-revised form 27 September 2006.

Published, JLR Papers in Press, October 2, 2006.
DOI 10.1194/jlr.M600050-JLR200

Abbreviations: FALDH, fatty aldehyde dehydrogenase; MBP, maltose binding protein; MTBSTFA, *N*-methyl-*N*-(*tert*-butyldimethylsilyl)trifluoroacetamide; PPARα, peroxisome proliferator-activated receptor α.

[1] To whom correspondence should be addressed.
e-mail: s.ferdinandusse@amc.uva.nl

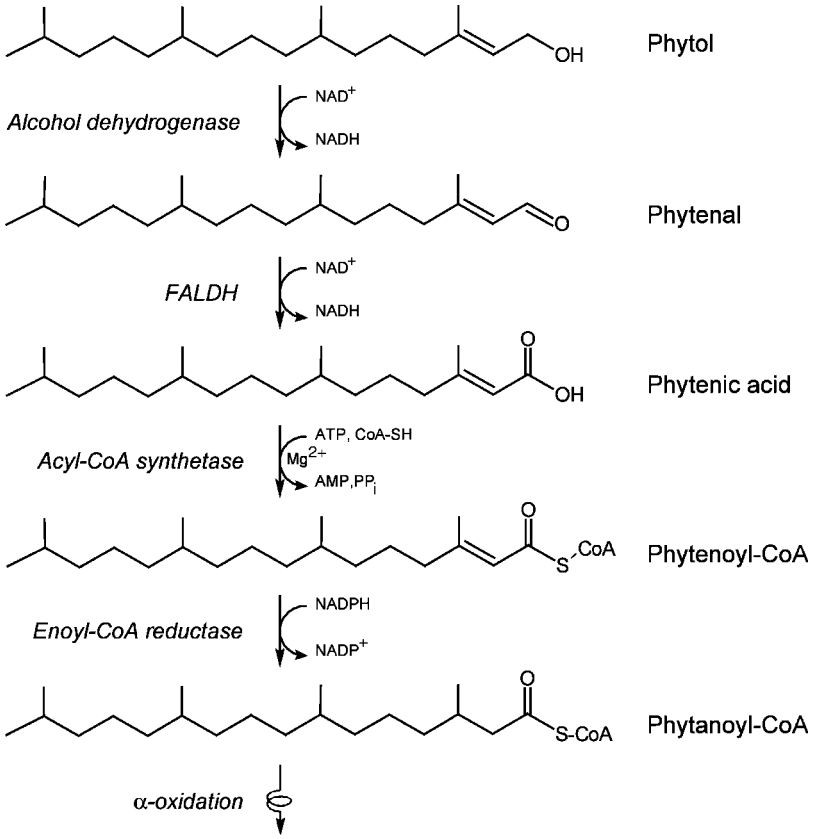

Fig. 1. Pathway of the metabolism of phytol to phytanic acid. Phytol is first converted into (*E*)-phytenic acid by the successive action of an unknown alcohol dehydrogenase and fatty aldehyde dehydrogenase (FALDH). Phytenic acid is then activated by a synthetase to produce (*E*)-phytenoyl-CoA and finally converted by an enoyl-CoA reductase into phytanoyl-CoA. Phytanoyl-CoA is further broken down by α-oxidation.

enzyme fatty aldehyde dehydrogenase (FALDH), which is encoded by the Aldehyde Dehydrogenase 3A2 gene (16). Recently, it was shown that phytenic acid is activated to its corresponding CoA ester, either at the endoplasmic reticulum or at the peroxisome, which is then reduced by a reductase converting phytenoyl-CoA to phytanoyl-CoA either in the peroxisome or at the mitochondrion (17).

In this study, we investigated the metabolism of phytol to phytanic acid in the mouse and the role of PPARα in its regulation. To this end, phytol concentrations were determined and the activities of the enzymes involved in phytol metabolism were analyzed in different tissues of wild-type and PPARα-deficient (PPARα$^{-/-}$) mice fed a phytol-enriched diet. To further investigate the role of PPARα, the activities of the enzymes involved in phytol metabolism were analyzed in different tissues of wild-type and PPARα$^{-/-}$ mice fed a diet enriched with Wy-14,643, a well-known synthetic PPARα agonist.

MATERIALS AND METHODS

Materials

Pelleted mouse chow without enrichments or enriched with 0.5% (w/w) phytol [mixture of (*E*)- and (*Z*)-phytol], 0.1% (w/w) Wy-14,643, or 0.1% (w/w) fenofibrate was purchased from Hope Farms (Woerden, The Netherlands). Phytol was from Merck (Darmstadt, Germany). Wy-14,643 was obtained from Tocris Bioscience (Ellisville, MO), and fenofibrate was from Sigma-Aldrich (St. Louis, MO). [$^2H_3$]phytanic acid was purchased from Dr. H. J. ten Brink (Free University Medical Center, Amsterdam, the Netherlands). C19-OH was obtained form Janssen Chimica (Beerse, Belgium). A mixture of (*E*)- and (*Z*)-phytenic acid was synthesized as described previously (18). Phytenoyl-CoA isomers were chemically synthesized from a mixture of (*E*)- and (*Z*)-phytenic acid as described (19). Methyl-β-cyclodextrin was purchased from Fluka (Buchs, Switzerland). NADPH, NAD$^+$, the first-strand cDNA synthesis kit for RT-PCR, and the LightCycler FastStart DNA Master SYBR Green I kit were obtained from Roche (Mannheim, Germany). *N*-Methyl-*N*-(*tert*-butyldimethylsilyl)-trifluoroacetamide (MTBSTFA) was obtained from Pierce (Rockford, IL). Silica gel columns were purchased from J. T. Baker (Philipsburg, NJ). *Escherichia coli* INVα cells and Trizol were obtained from Invitrogen (Carlsbad, CA). The pGEM-T vector was from Promega (Madison, WI). The pMAL-C2X vector and amylose-resin columns were purchased from New England Biolabs (Beverly, MA). Freund's complete and incomplete adjuvant were from Difco Laboratories (Detroit, MI). Goat anti-rabbit antibodies conjugated with alkaline phosphatase were obtained from Bio-Rad (Hercules, CA). Complete^{mini} tablets containing a cocktail of protease inhibitors were purchased from Roche (Basel, Switzerland). Nitrocellulose membrane was from Schleicher and Shuell (Keene, NH). Protifar was obtained from Nutricia (Zoetermeer, The Netherlands). All other chemicals were of analytical grade.

Animals

Male wild-type and PPARα$^{-/-}$ mice on a Sv/129 genetic background were used to study the effects of phytol and Wy-14,643 treatment (20), and male wild-type mice on a Swiss genetic background were used to study the effects of fenofibrate treatment. Six week old wild-type and PPARα$^{-/-}$ mice were fed pelleted mouse chow containing no (control) or 0.5% (w/w) phytol for 1 or 8 weeks. Each group consisted of three animals. Nine week old wild-type and PPARα$^{-/-}$ mice were fed pelleted mouse chow containing no or 0.1% (w/w) Wy-14,643 for 2 weeks. Each group consisted of three animals. Eight week old wild-type mice were fed pelleted mouse chow containing no or 0.1% (w/w) fenofibrate for 5 weeks. Each group consisted of five animals. At the end of the experiments, mice were anesthetized using isoflurane, and tissues were harvested. The animals were always euthanized at the same time of day, and they had free access to water and food until that moment. Tissues were snap-frozen in liquid nitrogen and stored at −80°C until further analysis. All animal experiments were approved by the University of Amsterdam Animals Experiments Committee.

Synthesis of phytenal

Phytenal was synthesized from its precursor phytol essentially as described previously (18). Briefly, phytol [a mixture of (*E*)- and (*Z*)-isomers] was oxidized to the corresponding aldehydes with CrO_3-pyridine in dry methylene chloride under a flow of nitrogen to exclude water and oxygen. The oxidant was prepared in 30 ml of dichloromethane (dried over anhydrous Na_2SO_4) by addition of 24 mmol of anhydrous pyridine, followed by 12 mmol of CrO_3 in small batches under magnetic stirring. After clearing of the initial turbidity, 2 mmol of phytol in 4 ml of dichloromethane was added. The mixture was stirred for 1 h. Subsequently, the solution was transferred into a separatory funnel and washed with aqueous 5% NaOH for elimination of the excess CrO_3, 5% HCl for the elimination of pyridine, 5% $NaHCO_3$ for neutralization, and finally saturated NaCl. After drying over anhydrous Na_2SO_4, the organic solvent was filtrated and evaporated under a flow of nitrogen. The residue was then purified over a silica gel column and eluted with chloroform, which was subsequently evaporated under a flow of nitrogen. Phytenal was stored in aliquots under argon at −80°C until use. GC-MS analysis of the product showed two peaks corresponding to the (*E*)- and (*Z*)-isomers of phytenal with a molecular ion at *m/z* 294 and a fragmentation pattern specific for aldehydes.

Phytol analysis in tissue homogenates

Tissue phytol levels were determined as described (13). Briefly, tissues were homogenized in PBS. C19-OH (10 μl of a 50 μM solution dissolved in ethanol) was added to 100 μl of tissue homogenate (5 mg/ml), and the sample was subjected to alkaline hydrolysis by adding 2 ml of 1 M NaOH in methanol for 45 min at 110°C. After cooling to room temperature, the pH was decreased by adding 480 μl of 37% HCl. Subsequently, phytol was extracted with 2 ml of hexane, and the organic layer was evaporated to dryness under nitrogen at 40°C. Samples were dissolved in 0.5 ml of heptane and purified on a silica gel column using 92:8 (v/v) heptane-diethyl ether as eluent. The eluate was evaporated to dryness under nitrogen at 40°C and derivatized with MTBSTFA and pyridine (50 μl each) at 80°C for 30 min. Samples were evaporated to dryness under nitrogen at 40°C, dissolved in 100 μl of hexane, and subjected to GC-MS analysis, essentially as described previously (21). The metabolites were quantified using a calibration curve of phytol.

Enzyme activity measurements

All enzyme activity measurements were performed in freshly prepared tissue homogenates. FALDH activity measurements in liver were performed essentially as described previously (21). Briefly, FALDH activity was measured with both phytol and phytenal as substrates. The reaction mixture consisted of liver protein (20 and 50 μg for phytol and phytenal incubations, respectively), 50 mM glycine buffer, pH 9.2, 1 mM NAD^+, 0.1% sodium cholate, and 1 mg/ml methyl-β-cyclodextrin in a total volume of 500 μl. Reactions were performed at 37°C and initiated by the addition of substrate in final concentrations of 200 and 150 μM for phytol and phytenal, respectively. After 10 min, the incubations were terminated by the addition of 50 μl of 2 M HCl. As internal standard, 50 pmol of [$^2H_3$]phytanic acid, dissolved in toluene, was added. Then, 2 ml of hexane was added, and after vigorous vortexing, the samples were centrifuged, after which the organic layer was evaporated to dryness under a stream of nitrogen at 40°C. After derivatization with MTBSTFA and pyridine (50 μl each) at 80°C for 30 min, the samples were evaporated to dryness under nitrogen at 40°C, dissolved in 200 μl of hexane, and subjected to GC-MS analysis as described previously (21).

Enzymatic activation of phytenic acid to its CoA ester was measured essentially as described previously (17). Briefly, tissue homogenate (8 μg of protein for liver homogenates, 10 μg of protein for kidney and heart homogenates, and 25 μg of protein for small intestine and brain homogenates) was incubated with a mixture containing 50 mM Tris, pH 8.0, 10 mM ATP, 10 mM $MgCl_2$, 0.5 mM CoA, 1 mg/ml methyl-β-cyclodextrin, and 100 μM phytenic acid [a mixture of (*E*)- and (*Z*)-phytenic acid] in a total volume of 100 μl. The incubation was allowed to proceed for 30 min when the activity was measured in liver and for 60 min in all other tissues. Reactions were terminated by the addition of 100 μl of acetonitrile and placed on ice. Samples were centrifuged for 10 min at 10,000 *g* at 4°C, and supernatants were analyzed by HPLC.

Reduction of phytenoyl-CoA to phytanoyl-CoA was determined essentially as described previously (17). Briefly, the reaction mixture contained 50 mM HEPES, pH 7.0, 1 mM NADPH, 40 μM phytenoyl-CoA [a mixture of (*E*)- and (*Z*)-phytenoyl-CoA], and tissue homogenate (25 μg for kidney homogenates, 100 μg for liver homogenates, and 200 μg for small intestine, heart, and brain homogenates) in a total volume of 100 μl. Reactions were started by the addition of substrate and incubated at 37°C for 15 min for liver homogenates and for 30 min for all other tissue homogenates. Reactions were terminated by the addition of 100 μl of acetonitrile and placed on ice. Samples were centrifuged for 10 min at 10,000 *g* at 4°C, and supernatants were analyzed by HPLC.

Quantitative real-time RT-PCR analysis

Total RNA was isolated from RNA*later*-treated mouse liver and kidney samples using Trizol extraction, after which cDNA was prepared using a first-strand cDNA synthesis kit for RT-PCR. Quantitative real-time PCR analysis of FALDH and β-actin in liver and kidney was performed using the LightCycler FastStart DNA Master SYBR Green I kit. The following primers were used for FALDH: forward, 5′-CATACTTACAGATGTTGATCC-3′; reverse, 5′-CTCCAAAGGGCAGAGAATTA-3′. Primers for β-actin were used as described (22). Melting curve analysis was carried out to confirm the generation of a single product. Amplification of a single product of the correct size was also confirmed by agarose gel electrophoresis. Duplicate analyses were performed for all samples. Data were analyzed using linear regression calculations as described by Ramakers et al. (23). To adjust for variations in the amount of input RNA, the values for FALDH were normalized against the values for the housekeeping gene β-actin.

Preparation of antibodies

A polyclonal antiserum was raised against an N-terminal peptide corresponding to amino acids 1–96 of human FALDH,

expressed as a fusion protein with maltose binding protein (MBP). The coding region for this peptide (bp 1–288) was amplified from human liver cDNA by PCR using the following primers: a *Bam*HI-tagged forward primer (5′-ggatccATGGAGCTCGAAGTCCGG-3′) and a *Sal*I-tagged reverse primer (5′-gtcgacTTAGGCCTCATCCAGCATGGTGAG-3′) (restriction sites are underlined). The resulting PCR product was ligated into the pGEM-T vector, and sequence analysis was performed to exclude sequence errors introduced by Taq polymerase. The fragment was subsequently cloned into the pMAL-C2X vector to create pMAL-FALDH-Nterm, using the *Bam*HI and *Sal*I restriction sites downstream of the isopropyl-1-thio-β-D-galactopyranoside-inducible promoter. The *E. coli* strain INVα was transformed with the expression plasmid pMAL-FALDH-Nterm. Transformed cells were grown at 37°C in 100 ml of Luria-Bertani medium supplemented with 0.2% (w/v) glucose and 100 μg/ml ampicillin to an optical density at 600 nm of ~0.6, and isopropyl-1-thio-β-D-galactopyranoside was added to a final concentration of 1 mM to induce expression of the fusion protein. Cells were lysed by sonication on ice (twice for 15 s at an output of 8 W, with an interval of 1 min). The MBP fusion protein was purified on amylose-resin columns according to the protocol of the manufacturer (New England Biolabs). MBP-FALDH-Nterm was subjected to preparative SDS-PAGE, isolated from the gel, and subsequently used to raise antibodies. To this end, a female New Zealand White rabbit was injected subcutaneously with 100 μg of the antigen mixed with an equal volume of Freund's complete adjuvant. After 1 month, the immunization was continued by booster injections (each containing 100 μg of antigen in Freund's incomplete adjuvant) until a satisfactory antibody titer was obtained.

Immunoblot analysis

Small pieces of tissue were homogenized in PBS containing a cocktail of protease inhibitors. Twenty micrograms of protein was separated on a 10% (w/v) SDS-polyacrylamide gel and transferred to a nitrocellulose membrane (24). After blocking of nonspecific binding sites with 30 g/l Protifar and 10 g/l BSA in 1 g/l Tween-20/PBS, the blot was incubated for 2 h with rabbit polyclonal antibodies raised against FALDH diluted 1:1,500 in 4% BSA in PBS. Goat anti-rabbit IgG antibodies conjugated to alkaline phosphatase were used for detection.

Statistical analyses

Data are expressed as means ± SD. Statistical significance was evaluated using an unpaired Student's *t*-test. The results were considered significant at $P < 0.01$.

RESULTS

Phytol accumulation

Phytol levels were measured in several tissues to investigate the distribution of phytol in different organs of the mouse after a phytol-enriched diet. As expected, no phytol could be detected in any of the tissues studied of mice receiving a control diet. In the liver and small intestine of mice fed a phytol-enriched diet, there was an accumulation of phytol, whereas no phytol could be detected in brain, heart, and kidney.

In **Fig. 2**, the amounts of (*Z*)- and (*E*)-phytol detected in liver and small intestine of wild-type and PPARα$^{-/-}$ mice are shown. The phytol levels in small intestine varied considerably between individual mice, most likely attributable to the fact that the animals were fed ad libitum until euthanized. Despite this high variance, the amount of (*E*)-phytol was higher in PPARα$^{-/-}$ mice than in wild-type animals (Fig. 2C).

In a previous study, we determined the phytol levels in liver and showed that after 4 weeks of diet the accumulation of phytol in PPARα$^{-/-}$ mice was more substantial than in wild-type animals (13). In this study, we determined the levels of both (*Z*)- and (*E*)-phytol in liver. After 1 week on a phytol-enriched diet, there were no significant differences in phytol levels between wild-type and PPARα$^{-/-}$ mice (Fig. 2). After 8 weeks on the phytol-enriched diet, however, the amount of (*E*)-phytol, in contrast to the (*Z*)-isomer, was increased significantly in PPARα$^{-/-}$ mice compared with wild-type animals. In wild-type mice, the phytol level did not increase with time, but it did increase in PPARα$^{-/-}$ mice.

Phytol-degrading enzymes in the liver

Because FALDH only converts (*E*)-phytenal into (*E*)-phytenic acid, the predominant accumulation of (*E*)-phytol in liver of PPARα$^{-/-}$ mice in combination with lower hepatic levels of phytanic acid in PPARα$^{-/-}$ mice compared with wild-type animals (13) suggests a decreased capacity of the phytol degradation pathway in PPARα$^{-/-}$ mice. To investigate this, we measured the activities of the enzymes of this pathway in liver (**Fig. 3**).

First, we measured the conversion of phytol and phytenal into (*E*)-phytenic acid. When phytol is used as a substrate, the first and second steps of the pathway are measured simultaneously (catalyzed by alcohol dehydrogenase and FALDH, respectively). Using phytenal as a substrate, only the second step catalyzed by FALDH is measured. The specific activity of (*E*)-phytenic acid formation measured with both substrates was higher in wild-type mice than in PPARα$^{-/-}$ mice. Under the influence of the phytol-enriched diet, both assays revealed significantly increased (*E*)-phytenic acid formation in wild-type mice (Fig. 3A). Because phytol metabolites are ligands for PPARα, this suggests that PPARα plays a role in the regulation of FALDH expression and might also be involved in the regulation of the expression of the alcohol dehydrogenase. Because the fold induction of the activity measured with phytol and phytenal as substrate was the same, it is probable that the reaction catalyzed by FALDH is the rate-limiting step. Interestingly, a small but significant induction of (*E*)-phytenic acid formation also was observed with both substrates in PPARα$^{-/-}$ mice, although this was much less pronounced compared with wild-type mice, indicating that there are both PPARα-dependent and -independent effects. Immunoblot analysis of FALDH showed a clear induction of FALDH protein in wild-type mice fed a phytol diet compared with the control diet, whereas no induction was observed in PPARα$^{-/-}$ mice (Fig. 3A). To substantiate that FALDH expression is under the control of PPARα, FALDH expression was studied in wild-type and PPARα$^{-/-}$ mice treated with the PPARα ligand Wy-14,643. Figure 3B shows that induction of FALDH protein indeed occurred in wild-

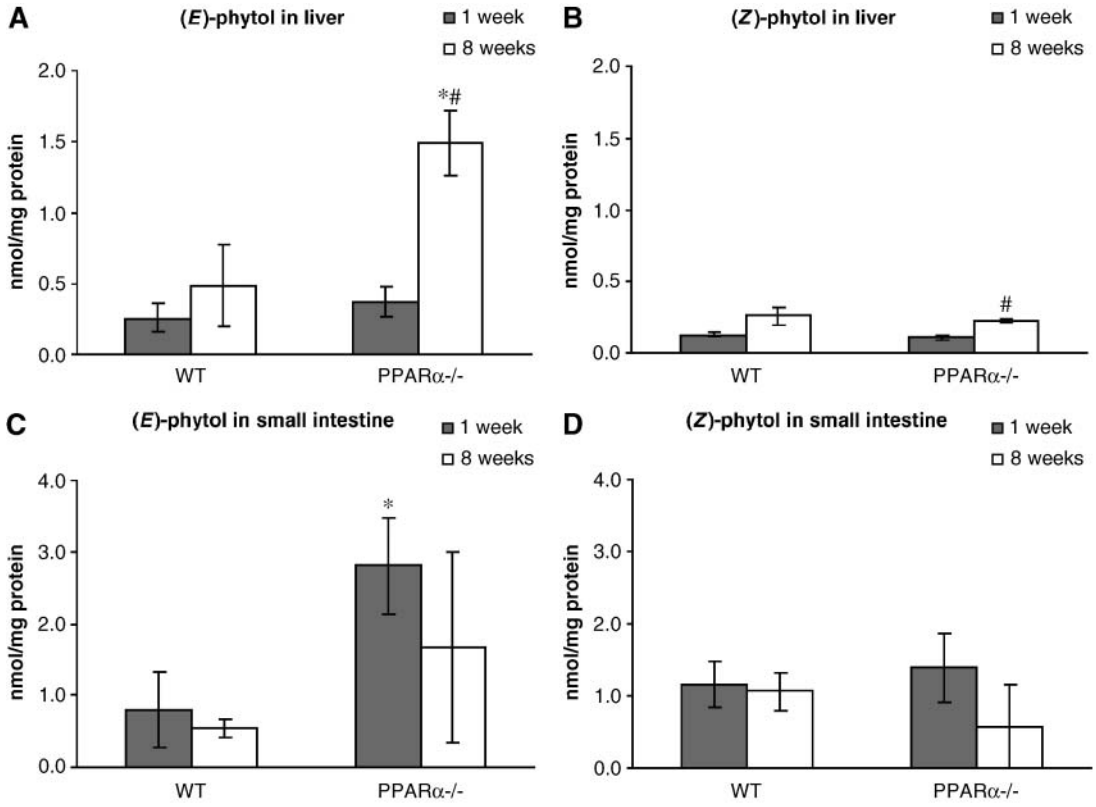

Fig. 2. Phytol accumulation in wild-type (WT) and peroxisome proliferator-activated receptor α-deficient (PPARα$^{-/-}$) mice fed a diet enriched with 0.5% phytol for 1 and 8 weeks. A: (*E*)-Phytol levels in liver. B: (*Z*)-Phytol levels in liver. C: (*E*)-Phytol levels in small intestine. D: (*Z*)-Phytol levels in small intestine. Values represent means of three animals per group ± SD. * $P < 0.01$ between wild-type and PPARα$^{-/-}$ mice after the same diet period; # $P < 0.01$ between 1 week and 8 weeks of phytol diet in mice of the same genotype.

type mice, but not in PPARα$^{-/-}$ animals, fed a diet enriched with Wy-14,643. Investigation of liver mRNA levels using quantitative RT-PCR showed a 3.0-fold induction of FALDH mRNA after Wy-14,643 treatment in wild-type mice. The induction of FALDH mRNA is in agreement with the mode of action of Wy-14,643, which activates PPARα to induce the transcription of its target genes.

Second, the activation of (*E*)-phytenic acid to its CoA ester was significantly increased in liver from phytol-fed and Wy-14,643-treated wild-type animals compared with animals on a control diet (Fig. 3C). The specific activity for the formation of (*Z*)-phytenoyl-CoA was 17-fold lower than for (*E*)-phytenoyl-CoA (**Table 1**), and although it was slightly higher in phytol-fed and Wy-14,643-treated wild-type mice, this difference was not statistically significant (data not shown). The increase in (*E*)-phytenoyl-CoA formation was not observed in PPARα$^{-/-}$ mice on a diet enriched with phytol or Wy-14,643, indicating that also the induction of phytenoyl-CoA synthetase is PPARα-dependent.

Third, the specific activity of phytenoyl-CoA reductase, the last step of the pathway, was significantly increased in wild-type mice on a phytol-enriched diet, whereas no induction was observed in PPARα$^{-/-}$ mice. This suggests that, in addition to phytenoyl-CoA synthetase, phytenoyl-CoA reductase is regulated in a PPARα-dependent manner. However, no induction of phytenoyl-CoA reductase activity was observed after feeding a Wy-14,643-enriched diet. The difference in phytenoyl-CoA reductase regulation between the phytol diet and Wy-14,643 treatment could be attributable to ligand-specific activation of PPARα or to the fact that phytenoyl-CoA reductase is not induced directly via PPARα activation but is induced in phytol-fed animals as a consequence of accumulating metabolites from the phytol breakdown pathway. To further investigate this, the effect of fenofibrate, another synthetic PPARα agonist, on phytenoyl-CoA reductase activity was investigated. Like Wy-14,643 treatment, fenofibrate treatment did not result in an increase of phytenoyl-CoA reductase activity in wild-type mice. The mean specific activity (±SD) measured in liver from five wild-type mice was 0.43 ± 0.12 nmol/mg/min, and the specific activity after fenofibrate treatment was 0.34 ± 0.03 nmol/mg/min. These results show that phytenoyl-CoA reductase is not induced directly via PPARα activation but that accumulating metabolites of the phytol breakdown pathway, which is upregulated after PPARα activation, cause an increase in phytenoyl-CoA reductase activity.

When studying the stereochemistry of the reductase reaction, the specific activity for the reduction of (*E*)-phytenoyl-CoA was found to be 2.8-fold higher than that for the purified (*Z*)-isomer (data not shown).

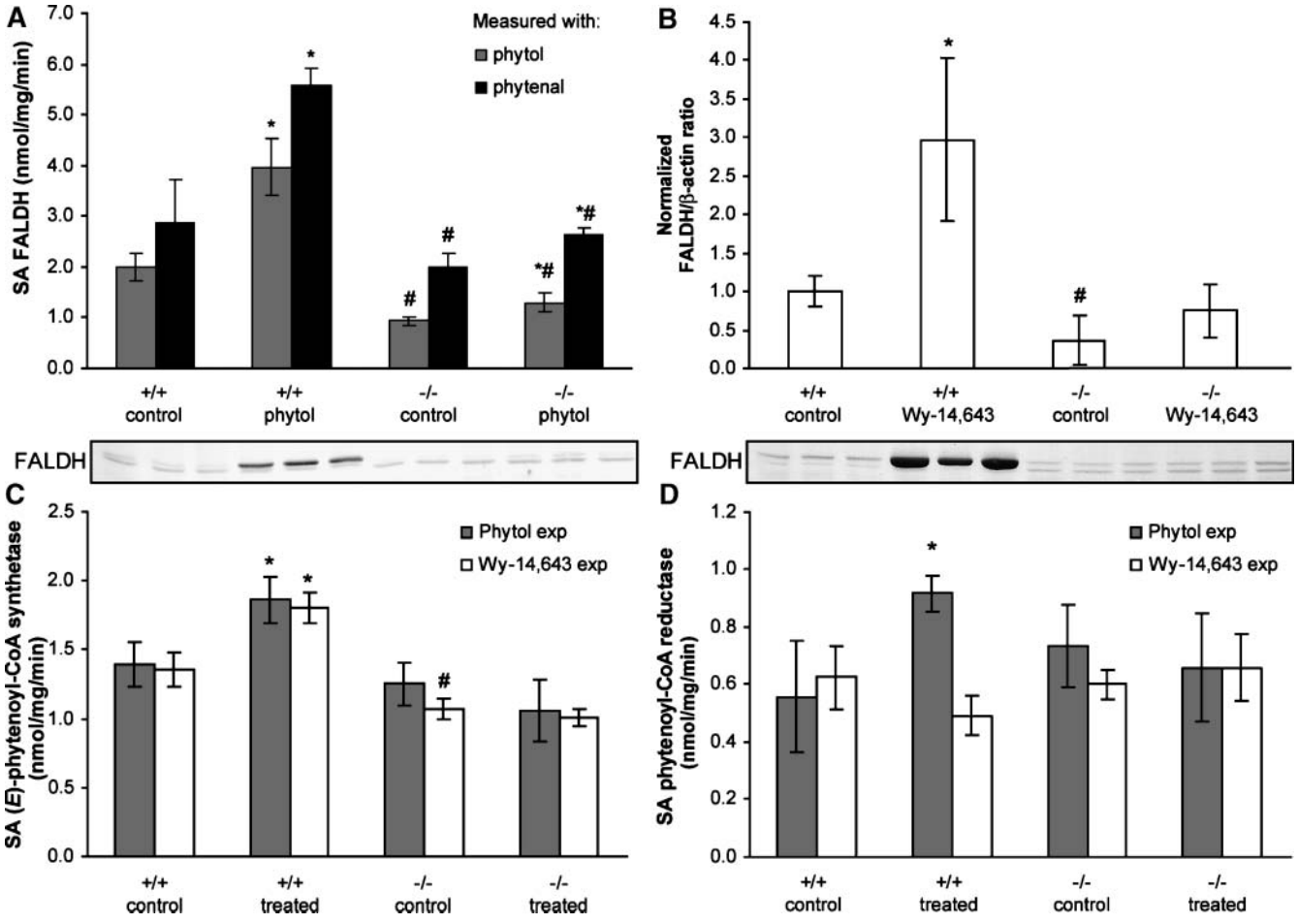

Fig. 3. Enzyme activity measurements and immunoblot analysis performed in liver homogenates of wild-type (+/+) and PPARα$^{-/-}$ (−/−) mice (three mice per group) on a control diet or either a phytol-enriched diet for 8 weeks or a Wy-14,643-enriched diet for 2 weeks. A: Upper panel, rates of phytenic acid production with phytol as a substrate (gray bars) or specific activity (SA) of FALDH with phytenal as a substrate (black bars) in mice on a control diet or a phytol-enriched diet. Lower panel, immunoblot analysis of FALDH in liver from wild-type and PPARα$^{-/-}$ mice on a control diet or a phytol-enriched diet. B: Upper panel, quantitative RT-PCR analysis of FALDH in liver from mice of both genotypes on a control diet or a Wy-14,643-enriched diet. Presented are the normalized FALDH/β-actin ratios. The level of FALDH mRNA in wild-type mice on a control diet was set to 1.0. Lower panel, immunoblot analysis of FALDH in wild-type and PPARα$^{-/-}$ mice on a control diet or a Wy-14,643-enriched diet. C: Phytenoyl-CoA synthetase activity in mice from both genotypes on a control diet or either a phytol-enriched diet or a Wy-14,643-enriched diet. D: Phytenoyl-CoA reductase activity in mice from both genotypes on a control diet or either a phytol-enriched diet or a Wy-14,643-enriched diet. Values represent means of three animals per group ± SD. * $P < 0.01$ between the phytol-/Wy-14,643-enriched diet and the control diet in mice of the same genotype; # $P < 0.01$ between PPARα$^{-/-}$ mice and wild-type mice on the same diet.

Site of phytol degradation

To gain more insight into the site of phytol metabolism in the body, we investigated the activities of the enzymes involved in this pathway in different mouse tissues. The tissue distribution of FALDH was described previously (25). Highest expression and activity were found in liver, followed by lung, kidney, small intestine, and stomach. Low but detectable FALDH expression and activity were also present in brain, skin, heart, and muscle. Immunoblot analysis of FALDH in kidney, heart, and brain homogenates is depicted in **Fig. 4A**. In heart and brain, FALDH protein levels are detectable, but no induction of FALDH protein was observed after the Wy-14,643-enriched diet. In kidney, however, FALDH protein was significantly induced in wild-type mice after the Wy-14,643-enriched diet, indicating regulation via PPARα. Analysis of FALDH mRNA levels in kidney (Fig. 4B) showed an induction of FALDH mRNA in wild-type mice after Wy-14,643 treatment but not in PPARα$^{-/-}$ mice, which is in agreement with the immunoblot results.

TABLE 1. Specific activities for the activation of (*E*)- and (*Z*)-phytenic acid to their corresponding CoA ester and for the reduction of phytenoyl-CoA in different tissues of wild-type mice on a control diet

Tissue	(*E*)-Phytenoyl-CoA Synthetase	(*Z*)-Phytenoyl-CoA Synthetase	Phytenoyl-CoA Reductase
		nmol/mg/min	
Liver	1.40 ± 0.02	0.08 ± 0.01	0.56 ± 0.04
Kidney	0.62 ± 0.09	0.10 ± 0.02	0.24 ± 0.12
Heart	0.72 ± 0.06	n.d.	0.03 ± 0.006
Small intestine	0.05 ± 0.03	n.d.	0.02 ± 0.006
Brain	0.12 ± 0.02	n.d.	0.04 ± 0.003

Values represent means ± SD (n = 3). n.d., not detectable.

In Table 1, both (*E*)- and (*Z*)-phytenoyl-CoA synthetase activities are shown. In all tissues tested, the specific activity

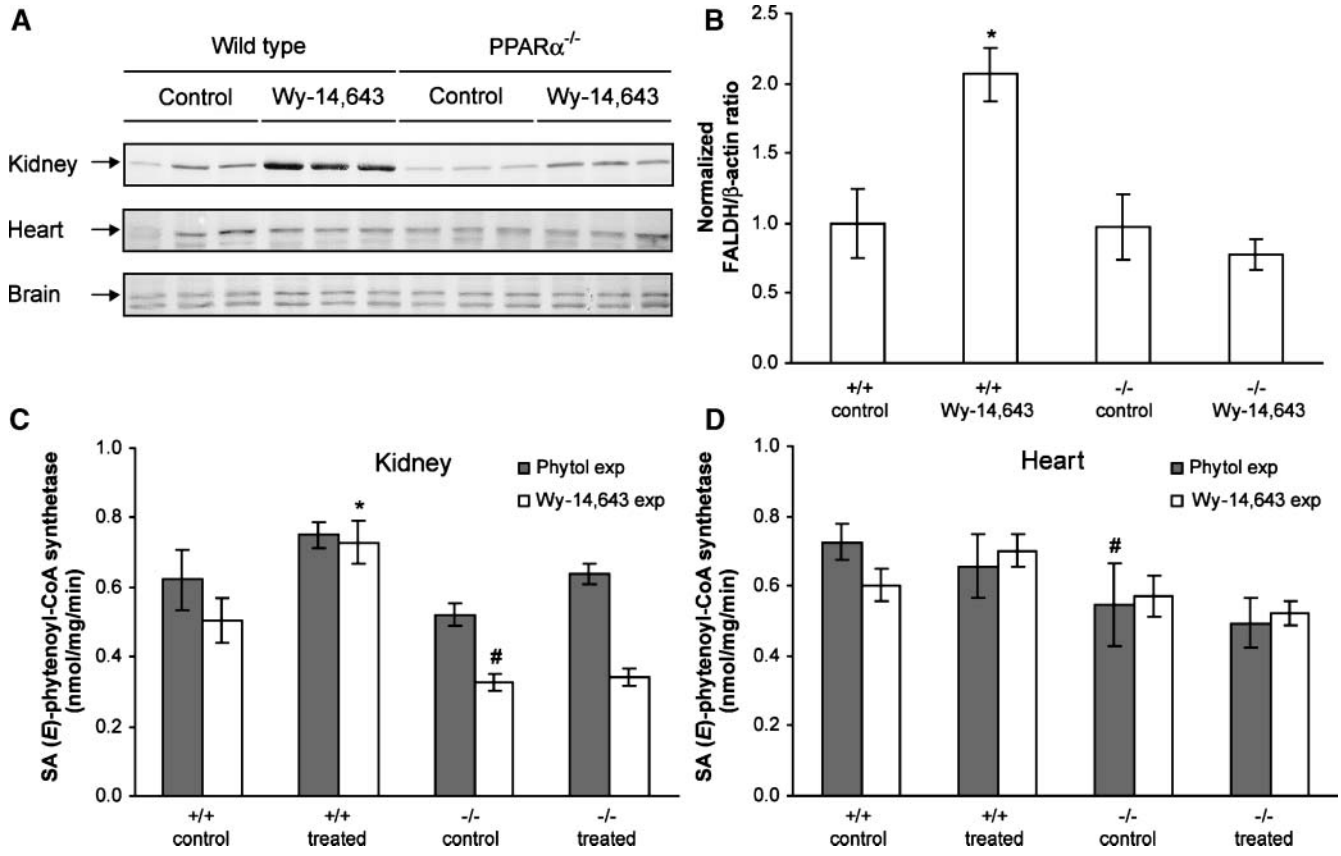

Fig. 4. Enzyme activity measurements and immunoblot analysis performed in kidney, heart, and brain homogenates of wild-type (+/+) and PPARα$^{-/-}$ (−/−) mice on a control diet or either a phytol-enriched diet for 8 weeks or a Wy-14,643-enriched diet for 2 weeks. A: Immunoblot analysis of FALDH in kidney, heart, and brain of wild-type and PPARα$^{-/-}$ mice on a control diet or a Wy-14,643-enriched diet (3 mice per group). B: Quantitative RT-PCR analysis of FALDH in kidney of mice from both genotypes on a control diet or a Wy-14,643-enriched diet. Presented are the normalized FALDH/β-actin ratios. The level of FALDH mRNA in wild-type mice on a control diet was set to 1.0. C: Phytenoyl-CoA synthetase specific activity (SA) in kidney of mice from both genotypes on a control diet or either a phytol-enriched diet or a Wy-14,643-enriched diet. D: Phytenoyl-CoA synthetase activity in heart of mice from both genotypes on a control diet or either a phytol-enriched diet or a Wy-14,643-enriched diet. Values represent means of three animals per group ± SD. * $P < 0.01$ between the phytol-/Wy-14,643-enriched diet and the control diet in mice of the same genotype; # $P < 0.01$ between PPARα$^{-/-}$ mice and wild-type mice on the same diet.

for the formation of (*E*)-phytenoyl-CoA was markedly higher than that for the (*Z*)-isomer. The highest activity of (*E*)-phytenoyl-CoA synthetase was measured in liver. In kidney and heart, the specific activity measured was approximately half of the value for liver. In small intestine and brain, very low specific activities of (*E*)-phytenoyl-CoA synthetase could be measured, whereas (*Z*)-phytenoyl-CoA synthetase activity was undetectable. In Fig. 4C, D, (*E*)-phytenoyl-CoA synthetase activities in kidney and heart of mice in the different feeding experiments are depicted. After treatment of wild-type mice with Wy-14,643, a significant increase of (*E*)-phytenoyl-CoA synthetase activity was observed in kidney. A slight increase of (*E*)-phytenoyl-CoA synthetase activity also was observed in heart of wild-type mice after treatment with Wy-14,643, but this was not significant. The increase observed in kidney of wild-type animals fed a phytol diet was also not significant. In other tissues, no change in (*E*)-phytenoyl-CoA synthetase activity was detected.

As for phytenoyl-CoA synthetase, the specific activity of phytenoyl-CoA reductase was highest in liver. In kidney, the specific activity was approximately half of the value for liver. In all other tissues tested, very low, but detectable, activities of phytenoyl-CoA reductase were measured (Table 1). In the extrahepatic tissues, phytenoyl-CoA reductase activity was not induced by phytol or by Wy-14,643.

DISCUSSION

Our results show that PPARα plays an important role in the regulation of the enzymes involved in phytol degradation. In livers from PPARα$^{-/-}$ mice, phytol was found to accumulate to much higher levels compared with livers from wild-type animals upon longer duration of the phytol-enriched diet, suggesting a decreased capacity for phytol metabolism in PPARα$^{-/-}$ mice compared with wild-type animals. Further investigation showed that the regulation of at least two of the four enzymes of this breakdown pathway (i.e., FALDH and phytenoyl-CoA synthetase) is PPARα-dependent, because their activities increase after phytol or Wy-14,643 feeding in livers from

wild-type mice but not from PPARα$^{-/-}$ animals. Only for FALDH was it reported previously that expression can be induced by the action of PPARα, although no functional peroxisome proliferator response element has been identified yet (26).

Both (*Z*)- and (*E*)-phytol are absorbed in the small intestine of the mouse, as shown by the presence of both isomers. Upon longer duration of the phytol-enriched diet, no increase in the accumulation of phytol was observed in small intestine. In contrast, the accumulation of phytol in the liver increased with time, which was mainly attributable to an increase in (*E*)-phytol levels. The predominant accumulation of the (*E*)-isomer of phytol strongly suggests that the phytol degradation pathway is stereospecific. Indeed, FALDH, which catalyzes the second step in the breakdown of phytol, exclusively forms (*E*)-phytenic acid. The third and fourth steps of the phytol degradation pathway, catalyzed by phytenoyl-CoA synthetase and phytenoyl-CoA reductase, respectively, also show a strong preference for (*E*)-isomers as substrate. The peroxisomal *trans*-2-enoyl-CoA reductase identified by Das, Uhler, and Hajra (27) was suggested as a putative candidate for the reduction of phytenoyl-CoA to phytanoyl-CoA (17). This reductase has been shown to be stereospecific toward the (*E*)-form of enoyl-CoA esters (17, 27) and has now been shown to convert (*E*)-phytenoyl-CoA to (*E*)-phytanoyl-CoA (28). It remains to be established, however, whether this enzyme is the sole reductase catalyzing the reduction of phytenoyl-CoA, especially because mitochondria, which lack the reductase identified by Das, Uhler, and Hajra (27), are also able to reduce phytenoyl-CoA. In conclusion, our results show that the phytol degradation pathway is stereospecific for the breakdown of (*E*)-phytol to phytanic acid.

All of the enzymes involved in the breakdown of phytol to phytanic acid displayed high activity in mouse liver. The first step, catalyzed by the alcohol dehydrogenase, cannot be measured directly, because the product of this reaction (i.e., phytenal) is very unstable. At least in liver, this enzyme must be present, because phytol was converted into (*E*)-phytenic acid in liver homogenates. The enzyme activity measurements of the other enzymes involved in the breakdown of phytol, together with the measurement of phytol levels in different tissues of the mouse, strongly suggest that the main site of phytol degradation is the liver. Phytol itself could be detected in liver and small intestine only after the phytol-enriched diet. Most likely, the phytol levels in small intestine are a reflection of the phytol that has been absorbed from the diet just before euthanasia. As a consequence, no increase in small intestinal phytol levels was observed with time, in contrast to the hepatic phytol concentration, which did increase with time.

In summary, the results described here show that the degradation of phytol to phytanic acid is regulated via PPARα. Furthermore, phytol accumulates almost exclusively in liver, and the enzymes involved in phytol degradation display their highest activities in liver, indicating that the liver is the main site of phytol metabolism in the body. Finally, the pathway shows specificity for the breakdown of (*E*)-phytol, because this isomer accumulates predominantly in liver of PPARα$^{-/-}$ mice on a phytol-enriched diet and at least three of the enzymes of the pathway have been shown to be stereospecific toward this isomer.

The authors thank R. Ofman for technical assistance and Prof. Dr. J. F. Rontani for advice. This work was supported by Grant 901-03-097 from the Netherlands Organization for Scientific Research (The Hague, The Netherlands) and by Grant QLG3-2002-00696 from the European Union.

REFERENCES

1. Hansen, R. P. 1966. Occurence of phytanic acid in rumen bacteria. *Nature.* **210:** 841.
2. Brown, P. J., G. Mei, F. B. Gibberd, D. Burston, P. D. Mayne, J. E. McClinchy, and M. Sidey. 1993. Diet and Refsum's disease. The determination of phytanic acid and phytol in certain foods and the application of this knowledge to the choice of suitable convenience foods for patients with Refsum's disease. *J. Hum. Nutr. Diet.* **6:** 295–305.
3. Wanders, R. J., G. A. Jansen, and O. H. Skjeldal. 2001. Refsum disease, peroxisomes and phytanic acid oxidation: a review. *J. Neuropathol. Exp. Neurol.* **60:** 1021–1031.
4. Wierzbicki, A. S., M. D. Lloyd, C. J. Schofield, M. D. Feher, and F. B. Gibberd. 2002. Refsum's disease: a peroxisomal disorder affecting phytanic acid alpha-oxidation. *J. Neurochem.* **80:** 727–735.
5. Monnig, G., J. Wiekowski, P. Kirchhof, J. Stypmann, G. Plenz, L. Fabritz, H. J. Bruns, L. Eckardt, G. Assmann, W. Haverkamp, et al. 2004. Phytanic acid accumulation is associated with conduction delay and sudden cardiac death in sterol carrier protein-2/sterol carrier protein-x deficient mice. *J. Cardiovasc. Electrophysiol.* **15:** 1310–1316.
6. Savolainen, K., T. J. Kotti, W. Schmitz, T. I. Savolainen, R. T. Sormunen, M. Ilves, S. J. Vainio, E. Conzelmann, and J. K. Hiltunen. 2004. A mouse model for alpha-methylacyl-CoA racemase deficiency: adjustment of bile acid synthesis and intolerance to dietary methyl-branched lipids. *Hum. Mol. Genet.* **13:** 955–965.
7. Steinberg, D., J. Avigan, C. E. Mize, J. H. Baxter, J. Cammermeyer, H. M. Fales, and P. F. Highet. 1966. Effects of dietary phytol and phytanic acid in animals. *J. Lipid Res.* **7:** 684–691.
8. Atshaves, B. P., H. R. Payne, A. L. McIntosh, S. E. Tichy, D. Russell, A. B. Kier, and F. Schroeder. 2004. Sexually dimorphic metabolism of branched-chain lipids in C57BL/6J mice. *J. Lipid Res.* **45:** 812–830.
9. Atshaves, B. P., A. L. McIntosh, H. R. Payne, J. Mackie, A. B. Kier, and F. Schroeder. 2005. Effect of branched-chain fatty acid on lipid dynamics in mice lacking liver fatty acid binding protein gene. *Am. J. Physiol. Cell Physiol.* **288:** C543–C558.
10. Verhoeven, N. M., R. J. Wanders, B. T. Poll-The, J. M. Saudubray, and C. Jakobs. 1998. The metabolism of phytanic acid and pristanic acid in man: a review. *J. Inherit. Metab. Dis.* **21:** 697–728.
11. Baes, M., S. Huyghe, P. Carmeliet, P. E. Declercq, D. Collen, G. P. Mannaerts, and P. P. van Veldhoven. 2000. Inactivation of the peroxisomal multifunctional protein-2 in mice impedes the degradation of not only 2-methyl-branched fatty acids and bile acid intermediates but also of very long chain fatty acids. *J. Biol. Chem.* **275:** 16329–16336.
12. Ellinghaus, P., C. Wolfrum, G. Assmann, F. Spener, and U. Seedorf. 1999. Phytanic acid activates the peroxisome proliferator-activated receptor alpha (PPARalpha) in sterol carrier protein 2-/sterol carrier protein x-deficient mice. *J. Biol. Chem.* **274:** 2766–2772.
13. Gloerich, J., N. van Vlies, G. A. Jansen, S. Denis, J. P. Ruiter, M. A. van Werkhoven, M. Duran, F. M. Vaz, R. J. Wanders, and S. Ferdinandusse. 2005. A phytol-enriched diet induces changes in fatty acid metabolism in mice both via PPARalpha-dependent and - independent pathways. *J. Lipid Res.* **46:** 716–726.
14. Heim, M., J. Johnson, F. Boess, I. Bendik, P. Weber, W. Hunziker, and B. Fluhmann. 2002. Phytanic acid, a natural peroxisome proliferator-activated receptor (PPAR) agonist, regulates glucose metabolism in rat primary hepatocytes. *FASEB J.* **16:** 718–720.

15. Zomer, A. W., B. van der Burg, G. A. Jansen, R. J. Wanders, B. T. Poll-The, and P. T. van der Saag. 2000. Pristanic acid and phytanic acid: naturally occurring ligands for the nuclear receptor peroxisome proliferator-activated receptor alpha. *J. Lipid Res.* **41:** 1801–1807.
16. Van den Brink, D. M., J. N. van Miert, G. Dacremont, J. F. Rontani, G. A. Jansen, and R. J. Wanders. 2004. Identification of fatty aldehyde dehydrogenase in the breakdown of phytol to phytanic acid. *Mol. Genet. Metab.* **82:** 33–37.
17. Van den Brink, D. M., J. N. van Miert, G. Dacremont, J. F. Rontani, and R. J. Wanders. 2005. Characterization of the final step in the conversion of phytol into phytanic acid. *J. Biol. Chem.* **280:** 26838–26844.
18. Rontani, J. F., P. C. Bonin, and J. K. Volkman. 1999. Biodegradation of free phytol by bacterial communities isolated from marine sediments under aerobic and denitrifying conditions. *Appl. Environ. Microbiol.* **65:** 5484–5492.
19. Rasmussen, J. T., T. Borchers, and J. Knudsen. 1990. Comparison of the binding affinities of acyl-CoA-binding protein and fatty-acid-binding protein for long-chain acyl-CoA esters. *Biochem. J.* **265:** 849–855.
20. Lee, S. S., T. Pineau, J. Drago, E. J. Lee, J. W. Owens, D. L. Kroetz, P. M. Fernandez-Salguero, H. Westphal, and F. J. Gonzalez. 1995. Targeted disruption of the alpha isoform of the peroxisome proliferator-activated receptor gene in mice results in abolishment of the pleiotropic effects of peroxisome proliferators. *Mol. Cell. Biol.* **15:** 3012–3022.
21. Van den Brink, D. M., J. M. van Miert, and R. J. Wanders. 2005. Assay for Sjogren-Larsson syndrome based on a deficiency of phytol degradation. *Clin. Chem.* **51:** 240–242.
22. Sousa, M. M., S. Du Yan, R. Fernandes, A. Guimaraes, D. Stern, and M. J. Saraiva. 2001. Familial amyloid polyneuropathy: receptor for advanced glycation end products-dependent triggering of neuronal inflammatory and apoptotic pathways. *J. Neurosci.* **21:** 7576–7586.
23. Ramakers, C., J. M. Ruijter, R. H. Deprez, and A. F. Moorman. 2003. Assumption-free analysis of quantitative real-time polymerase chain reaction (PCR) data. *Neurosci. Lett.* **339:** 62–66.
24. Laemmli, U. K. 1970. Cleavage of structural proteins during the assembly of the head of bacteriophage T4. *Nature.* **227:** 680–685.
25. Lin, Z., G. Carney, and W. B. Rizzo. 2000. Genomic organization, expression, and alternate splicing of the mouse fatty aldehyde dehydrogenase gene. *Mol. Genet. Metab.* **71:** 496–505.
26. Mandard, S., M. Muller, and S. Kersten. 2004. Peroxisome proliferator-activated receptor alpha target genes. *Cell. Mol. Life Sci.* **61:** 393–416.
27. Das, A. K., M. D. Uhler, and A. K. Hajra. 2000. Molecular cloning and expression of mammalian peroxisomal trans-2-enoyl-coenzyme A reductase cDNAs. *J. Biol. Chem.* **275:** 24333–24340.
28. Gloerich, J., J. P. Ruiter, D. M. van den Brink, R. Ofman, S. Ferdinandusse, and R. J. Wanders. 2006. Peroxisomal trans-2-enoyl-CoA reductase is involved in phytol degradation. *FEBS Lett.* **580:** 2092–2096.